

Plantazolicin, a Novel Microcin B17/Streptolysin S-Like Natural Product from *Bacillus amyloliquefaciens* FZB42[∇]

Romy Scholz,¹ Katie J. Molohon,² Jonny Nachtigall,³ Joachim Vater,³ Andrew L. Markley,⁴ Roderich D. Süssmuth,³ Douglas A. Mitchell,^{2,5,6*} and Rainer Borriss^{1*}

*Institut für Biologie/Bakteriengenetik, Humboldt-Universität zu Berlin, 10115 Berlin, Germany*¹; *Department of Microbiology, University of Illinois at Urbana-Champaign, Urbana, Illinois 61801*²; *Institut für Chemie, Technische Universität Berlin, 10623 Berlin, Germany*³; *Department of Chemistry and Biochemistry, University of California, San Diego, La Jolla, California 92093*⁴ and *Department of Chemistry*⁵ and *Institute for Genomic Biology,*⁶ *University of Illinois at Urbana-Champaign, Urbana, Illinois 61801*

Received 6 July 2010/Accepted 11 October 2010

Here we report on a novel thiazole/oxazole-modified microcin (TOMM) from *Bacillus amyloliquefaciens* FZB42, a Gram-positive soil bacterium. This organism is well known for stimulating plant growth and biosynthesizing complex small molecules that suppress the growth of bacterial and fungal plant pathogens. Like microcin B17 and streptolysin S, the TOMM from *B. amyloliquefaciens* FZB42 undergoes extensive posttranslational modification to become a bioactive natural product. Our data show that the modified peptide bears a molecular mass of 1,335 Da and displays antibacterial activity toward closely related Gram-positive bacteria. A cluster of 12 genes that covers ~10 kb is essential for the production, modification, export, and self-immunity of this natural product. We have named this compound plantazolicin (PZN), based on the association of several producing organisms with plants and the incorporation of azole heterocycles, which derive from Cys, Ser, and Thr residues of the precursor peptide.

Bacillus amyloliquefaciens FZB42 is a Gram-positive, plant growth-promoting bacterium with an impressive capacity to produce secondary metabolites with antimicrobial activity (7). The nonribosomal syntheses of polyketides (bacillaene, difficidin, and macrolactin), lipopeptides (surfactin, fengycin, and bacillomycin D), and siderophores (bacillibactin and the product of the *nrs* cluster) are carried out by large gene clusters distributed over the entire genome of *B. amyloliquefaciens* FZB42. While these compounds are biosynthesized in a 4'-phosphopantetheine transferase (Sfp)-dependent fashion, the production of the antibacterial dipeptide bacilysin is independent of Sfp (8, 9). In total, 8.5% of the entire genomic capacity of *B. amyloliquefaciens* FZB42 is devoted to the nonribosomal synthesis of secondary metabolites, exceeding that of the model Gram-positive bacterium *Bacillus subtilis* 168 by more than 2-fold (6). Prophage sequences that often harbor biosynthetic gene clusters of ribosomally synthesized peptides (microcins, lantibiotics/lantipeptides), which are common in *B. subtilis* strains, were not previously detected within the FZB42 genome. However, the presence of an antimicrobial compound(s) active against *sigW* mutant strain HB0042 of *B. subtilis* has been reported. SigW is an extracytoplasmic sigma factor that provides intrinsic resistance to antimicrobial compounds produced by other *Bacilli* (4).

The driving force for the current report was the finding that

FZB42 mutant RS6, which is deficient in the Sfp-dependent synthesis of lipopeptides and polyketides and in Sfp-independent bacilysin production (9), still produced an antibacterial substance active against *Bacillus subtilis* HB0042. This finding underscores the diversity of biosynthetic strategies employed by FZB42 and offers new possibilities for discovering novel natural products with biomedically relevant activities. Recent genomic analysis of FZB42 revealed a ribosomally encoded biosynthetic gene cluster that is conserved among many species across two domains of life (23). This cluster encodes a small precursor peptide that is posttranslationally modified to contain thiazole and (methyl)oxazole heterocycles (Fig. 1). These rings are derived from Cys and Ser/Thr residues through the action of a trimeric “BCD” synthetase complex, which consists of a cyclodehydratase (C), a dehydrogenase (B), and a docking protein (D) (23). This mechanism of modification is utilized in the biosynthetic pathways for streptolysin S (SLS, from *Streptococcus pyogenes*) (12), microcin B17 (24), the patellamides (33), and the thiopeptides (18, 25, 27, 39). The products of these clusters have been collectively classified as thiazole/oxazole-modified microcins (TOMMs) due to their genetic and chemical structure conservation (14).

During TOMM biosynthesis, the precursor peptide is bound by the BCD synthetase complex through specific motifs within the N-terminal leader sequence (26, 31). After substrate recognition, heterocycles are synthesized on the C-terminal core peptide over two enzymatic steps. The first is carried out by a cyclodehydratase, which converts Cys and Ser/Thr residues into the corresponding thiazolines and (methyl)oxazolines. A dehydrogenase then oxidizes the “azoline” rings to yield “azole” rings [thiazoles and (methyl)oxazoles], resulting in a net loss of 20 Da. The completion of TOMM biosynthesis includes the incorporation of ancillary

* Corresponding author. Mailing address for D. A. Mitchell: 1206 W. Gregory Drive, 3105 Institute for Genomic Biology, University of Illinois, Urbana, IL 61801. Phone: (217) 333-1345. Fax: (217) 333-0508. E-mail: douglasm@illinois.edu. Mailing address for R. Borriss: Institut für Biologie, Humboldt-Universität zu Berlin, Chausseestrasse 117, D-10115 Berlin, Germany. Phone: 49-30-2093-8137. Fax: 49-30-2093-8127. E-mail: rainer.borriss@rz.hu-berlin.de.

[∇] Published ahead of print on 22 October 2010.

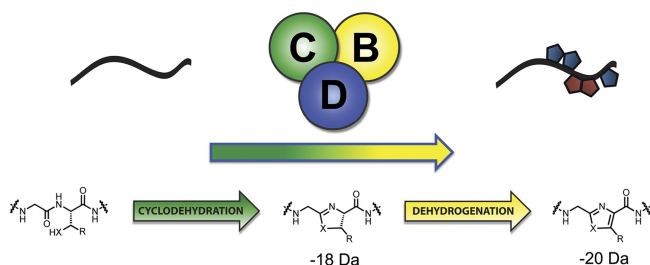


FIG. 1. Thiazole/oxazole-modified microcin (TOMM) biosynthesis. Through the action of a trimeric “BCD” complex, consisting of a cyclodehydratase (C, green), dehydrogenase (B, yellow), and docking/scaffolding protein (D, blue), thiazoles and (methyl)oxazoles are incorporated onto a peptidic scaffold (black). These heterocycles are synthesized from serine/threonine ($X = O$; $R = H/CH_3$) and cysteine ($X = S$; $R = H$) residues of the inactive precursor peptide and yield a bioactive natural product. The chemical transformations carried out by the cyclodehydratase and the dehydrogenase are shown, along with the corresponding mass change from the parent peptide in daltons.

modifications (e.g., dehydrations, methylations, macrocyclization, etc.) and leader peptide proteolysis (12, 18, 25, 27, 39). In many cases, the fully mature TOMM natural product is then actively exported from the cell through the use of an ABC

transport system. In this work, we describe the discovery, production, isolation, and initial genetic and chemical characterization of a novel TOMM from *B. amyloliquefaciens* FZB42. This natural product compound has a molecular mass of 1,335 Da (cpd1335) and has been named plantazolicin (PZN).

MATERIALS AND METHODS

Strain construction. The *B. amyloliquefaciens* strains and plasmids used in this study are summarized in Table 1. *Bacillus* and indicator strains were cultivated routinely on Luria-Bertani broth (LB) medium solidified with 1.5% agar. For production of PZN, a medium containing 40 g soy peptone, 40 g dextrin 10, 1.8 g KH_2PO_4 , 4.5 g K_2HPO_4 , 0.3 g $MgSO_4 \cdot 7H_2O$, and 0.2 ml KellyT trace metal solution per liter was used. KellyT trace metal solution contains 25 mg EDTA disodium salt dihydrate, 0.5 g $ZnSO_4 \cdot 7H_2O$, 3.67 g $CaCl_2 \cdot 2H_2O$, 1.25 g $MnCl_2 \cdot 4H_2O$, 0.25 g $CoCl_2 \cdot 6H_2O$, 0.25 g ammonium molybdate, 2.5 g $FeSO_4 \cdot 7H_2O$, and 0.1 g $CuSO_4 \cdot 5H_2O$ adjusted to pH 6 with NaOH, 500 ml H_2O .

The media and buffers used for DNA transformation of *Bacillus* cells were prepared according to Kunst and Rapoport (21). Competent cells were prepared as previously described (19). Mutants were obtained after transformation of the FZB42 derivatives with linearized, integrative plasmids containing resistance cassettes flanked by DNA regions homologous to the FZB42 chromosome. The oligonucleotides used for strain construction are listed in Table 2. Spectinomycin (90 $\mu g/ml$) was used for selecting transformants. Gene interruption strains were obtained as follows. For *pznB* RS26, a 2.7-kb PCR fragment was amplified from FZB42 chromosomal DNA using primers *pznB-fw* and *pznB-rv*. The fragment

TABLE 1. Bacterial strains and plasmids used in this study

Strain or plasmid	Description	Source or reference
Strains		
<i>Bacillus subtilis</i>		
DSM10 ^T	168 <i>trpC2</i> , type strain	DSMZ, Braunschweig, Germany
CU1065	168 <i>trpC2 attSPβ</i>	4
HB0042	168 <i>trpC2 attSPβ sigW::kan</i>	4
<i>Bacillus megaterium</i>		
7A/1	Indicator strain for polyketides	Laboratory stock
<i>Bacillus amyloliquefaciens</i>		
FZB42	Wild type	17
CH5	FZB42 <i>sfp::ermAM yczE::cm</i>	5
RSpMarA2	Insertion of pMarA in CH5: <i>degU::kan</i>	This work
RS6	<i>sfp::ermAM bac::cmR</i> , deficient in lipopeptides, polyketides, and bacilysin	9
RS26 ($\Delta pznB$)	RS6 $\Delta RBAM_007480::spc$, does not produce PZN	This work
RS27 ($\Delta pznI$)	RS6 $\Delta RBAM_007440::spc$, produces PZN	This work
RS28 ($\Delta pznJ$)	RS6 $\Delta RBAM_007450::spc$, does not produce PZN	This work
RS29 ($\Delta pznF$)	RS6 $\Delta RBAM_007400::spc$, produces PZN	This work
RS31 ($\Delta pznC$)	RS6 $\Delta RBAM_007460::spc$, does not produce PZN	This work
RS32 ($\Delta pznA$)	RS6 $\Delta pznA::spc$, does not produce PZN	This work
RS33 ($\Delta pznL$)	RS6 $\Delta RBAM_007500::spc$, produces desmethyl-PZN, 1,308 Da	This work
Plasmids		
pGEM-T	Ap ^r <i>lacZ'</i>	Promega
pMarA	Plasmid containing <i>mariner</i> transposon TnYLB-1	22
pIC333	Plasmid with <i>spc</i> cassette	T. Msadek, Institute Pasteur, Paris, France
pRS26a	pGEM-T with 2,700-bp <i>pznB</i>	This work
pRS26b	pGEM-T with <i>pznB::spc</i>	This work
pRS27	pGEM-T with SOE fusion product RBAM_007440- <i>spc</i>	This work
pRS28	pGEM-T with SOE fusion product RBAM_007450- <i>spc</i>	This work
pRS29	pGEM-T with SOE fusion product RBAM_007400- <i>spc</i>	This work
pRS31a	pGEM-T with 2,600-bp <i>pznC</i>	This work
pRS31b	pGEM-T with <i>pznC::spc</i>	This work
pRS32a	pGEM-T with 2,300-bp flanking region <i>pznA</i>	This work
pRS32b	pGEM-T with <i>pznA::spc</i>	This work

TABLE 2. Oligonucleotides used for gene replacement and SOE PCR

Oligonucleotide	Sequence (5' to 3')
Spectinomycin resistance cassettes	
spc-fw.....	CTCAGTGGAACGAAAACCTCACG
spc-rv.....	TAAGGTGGATACACATCTTGTC
pRS26a/b	
pznB-fw.....	ATCCATATCGCCAATCATACGG
pznB-rv.....	GGAATCAATACCTGTCAGTTCC
pRS31a/b	
pznD-fw.....	ATTGACTAGGAGGTATTGGACG
pznD-rv.....	TTCTATTGAATAGGAGGAGGCG
pRS32a/b	
007400cst-fw.....	TGGAATGCTCTTTCCGACGATC
007400cst-rv.....	GTAACCTCTGTTTCCACGTAACC
Primers for SOE PCR	
7400 rv.....	TCTTCATCACGCAAATCAGTGC
7400 fw.....	CCGCATAAACGGGAATTGGAAG
spc in 7410.....	TCTATAGAAACTTCTCAATTAGAAAAGAAAAGGGCAAGGAAATGAG
7410 in the spc.....	ACTCATTTCCCTTGCCCTTTTCTTTCTAATTGAGAGAAGTTTCTATAG
Start site in the spc.....	CTTTGTA AAAAGAGGAGCCTGTCTTATGAGCAATTTGATTAACGG
spc in start site.....	TTTTTCCGTTAATCAAATTTGCTCATAAGACAGGCTCCTCTTTTACAAAAG
7430 in the spc.....	GCTGGACTAAAAGGAGAGCGGGAATGAGCAATTTGATTAACGG
spc in ORF2.....	TTCTATAGAAACTTCTCAATTAGATTTAATATAAAGAAGCATAGACC
spc in 7430.....	TTTTTCCGTTAATCAAATTTGCTCATTCCCGCTCCTTTTAGTCCCAGC
ORF2 in the spc.....	TGGTCTATGCTTCTTATATATAAATCTAATTGAGAGAAGTTTCTATAG
7440 rv.....	TCACGTCCAATACCTCCTAGTC
7440 fw.....	ATCGACAGAGGGCAGATTATCG
ORF2 in the spc for 7450 fw.....	GATTATTGACTAGGAGGTATTGGACATGAGCAATTTGATTAACGG
7460 in the spc for 7450 rv.....	GTTTGTGAGACATCTGTATTCCTCCCTAATTGAGAGAAGTTTCTATAG
7450 rv.....	TAATGTGCTCCATTTACTCACC
7450 fw.....	TTGGCTCGAATAAATGTTGACC
spc in ORF2 for 7450 rv.....	TTTTTCCGTTAATCAAATTTGCTCATGTCCAATACCTCCTAGTCAATAATC
spc in 7460 for 7450 fw.....	TTCTATAGAAACTTCTCAATTAGGGAGGAATACAGATGTCTCAACAAAC
End site in the spc for 7500 rv.....	CGCTTAGACCCTAAAGATATACTTTCTCAATTGAGAGAAGTTTCTATAG
7490 in the spc for 7500 fw.....	AACTCTTTGGAGGTGTCACAGTTATATGAGCAATTTGATTAACGG
7500 fw.....	AAGTCCCTAGACGCCCTATTCC
7500 rv.....	GATGTGTAGTTTTCAACGCTCG
spc in the end site for 7500 fw.....	CTATAGAAACTTCTCAATTAGAGAAAGTATATCTTTAGGGTCTAAGCG
spc in 7490 for 7500 rv.....	CCGTTAATCAAATTTGCTCATATAACTGTGACACCTCCAAAGAGTTTACC
Primers for RT-PCR	
<i>pznF</i> (fw and rv).....	GGATTATTGCGTACTCCGTTTC, CTGCTCCGCCAATAAATG
<i>pznK</i> (fw and rv).....	ATGCCAAAGTACGGTTGGG, CTCCTGTAGGCTGCTTTCC
<i>pznG</i> (fw and rv).....	CCACAGGATATCAGCCTTGAAG, CGATAATCTGCCCTGTGTCG
<i>pznH</i> (fw and rv).....	CGCTCGCTCAAATTGAAACG, ACAACAACCCACAGATACGC
<i>pznI</i> (fw and rv).....	TAGCCTGGAAGCAGAGGGTA, ACTTTTGGCAGGTGACAACC
<i>pznA</i> (fw and rv).....	GGAGGAGTAAACAATTATGACTCAA, GTACAGGTACAGCGTGCAG
<i>pznJ</i> (fw and rv).....	TTGGATATCGGAATCGAGTTG, CGGATGCCAATTATCTGTT
<i>pznC</i> (fw and rv).....	TCATGTCCCTTGTTGTGTG, GCCGTGATACCATACTTGAGG
<i>pznD</i> (fw and rv).....	CGCGATGTAGATGACGTTTG, GATTGGCGATATGGATTAGTTG
<i>pznB</i> (fw and rv).....	AAGGCATGCCACTAATTTGG, GATAAAGAGTCCGCGAGAA
<i>pznE</i> (fw and rv).....	CATAGCAATAATGCGTACGGTG, GAGACATTGTGCGGCAAGA
<i>pznL</i> (fw and rv).....	GATGAGAGGGAAACCTCATCC, CTCCAAACTGTTCTCTGTC

was then cloned into pGEM-T, yielding plasmid pRS26a. Plasmid pRS26b was obtained by insertion of a spectinomycin resistance cassette (spc), which was subcloned by PCR using the spc-fw and spc-rv primers and the pIC333 plasmid as a template. The cassette was placed into the central region of the insert and digested with BglII and BamHI. For *pznC* RS31, a 2.6-kb fragment containing *pznC* was amplified by PCR with primers pznC-fw and pznC-rv and cloned into vector pGEM-T-Easy, yielding plasmid pRS31a. A central fragment of the insert was removed by digestion with Eco105I and replaced with the spectinomycin resistance cassette, yielding pRS31b. For *pznA* RS32, a 2.3-kb fragment encoding the unannotated precursor peptide *pznA* was amplified by PCR with primers 007400cst-fw and 007400cst-rv and cloned into vector pGEM-T-Easy, yielding

plasmid pRS32a. The precursor peptide gene was cleaved by Bsp1407I and interrupted by insertion of a spectinomycin resistance cassette, yielding pRS32b. The mutants RS27, RS28, RS29, and RS33 were generated by gene splicing using the splicing by overlapping extension (SOE) method (16). This method assists in avoiding possible polar effects caused by interrupted reading frames. SOE PCR fusion products were generated using the primers listed in Table 2 and the spectinomycin gene of pIC333. A-tailing of the *Pfu* PCR product was performed according to the Promega pGEM-T protocol and ligated into pGEM-T, yielding pRS27, pRS28, and pRS29. For mutant RS33, the PCR product was used directly for transformation.

Mutant RSpMarA2 was isolated from a *mariner*-based (pMarA) transposon

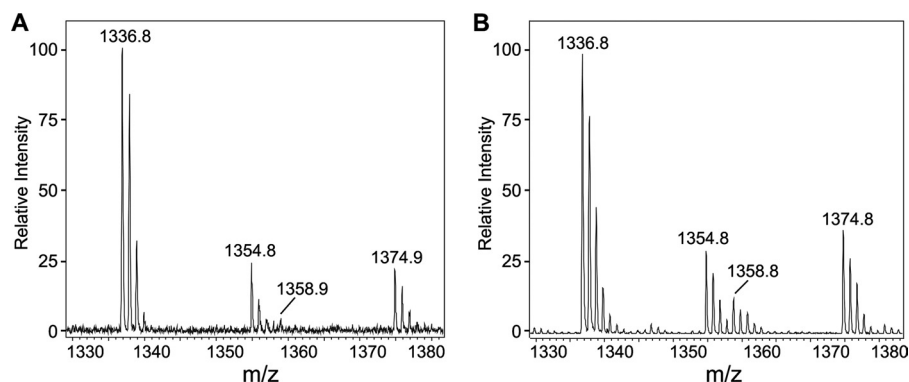


FIG. 2. MALDI-TOF mass spectra of *B. amyloliquefaciens* surface extracts. The samples were prepared from FZB42 (A) and RS6 (B) cells. Surface extracts were prepared and measured as described in Materials and Methods. Peaks at 1,336.8 $[M + H]^+$, 1,354.8 $[M + H_2O + H]^+$, 1,358.8 $[M + Na]^+$, and 1,374.8 $[M + K]^+$ Da indicate the presence of PZN in the wild-type strain (A) and in the Δ *sfp* Δ *bac* mutant strain RS6 (B).

library prepared in strain CH5 according to Le Breton et al. (22). In this transposon mutant, pMarA was integrated into the *degU* gene, which is a global transcriptional regulator that activates the bacillomycin D promoter (20). Coincidentally, we observed by high-performance liquid chromatography (HPLC)–electrospray ionization mass spectrometry (ESI-MS) that PZN is overproduced by this strain (see Fig. 3A).

Bioassay. LB agar (20 ml) was mixed with 0.5 ml of the indicator strain (optical density at 600 nm $[OD_{600}]$, ~ 1.0). Ten microliters of purified PZN suspended in water was spotted on the agar and incubated for 16 h at 22°C. The growth suppression activity of PZN was observed as a clear zone.

Cell surface extract. The extract was prepared in the following way. RSpMarA2 and RS26 were grown using production medium containing 1.5% agar for 24 h at 37°C. Cells were removed from the plates and treated with 50 ml of 70% acetonitrile–30% water, with 0.1% formic acid. After centrifugation (7,000 rpm, 20 min, 22°C), the extract was passed through a 0.45- μ m filter and concentrated to 2 ml using a rotary evaporator. The extract was dialyzed overnight against 5 liters distilled water using a membrane with a 1-kDa cutoff (Zellultrans V; Roth).

HPLC–ESI-MS. Bacterial strains were grown for 24 h at 37°C on solid production media containing 1.5% agar. One square centimeter of the bacterial lawn culture was extracted with 50 μ l of 70% acetonitrile–30% water with 0.1% formic acid for 30 s with vortexing. After centrifugation (14,000 rpm, 5 min) the solution was analyzed by online HPLC (1100 series HPLC system; Agilent Technologies) coupled to a QTRAP 2000 mass spectrometer (Applied Biosystems). A sample of extract (4 μ l) was separated by HPLC using a Luna C₁₈, 100- Å , 50- by 1-mm column (Phenomenex) at a flow rate of 60 μ l/min and a linear gradient of 5% to 100% acetonitrile with 0.1% formic acid in 10 min. MS analysis was performed in positive ion mode. MS settings were as follows: the mass window was from 500 to 1,400 Da, ion spray voltage was 4,500, and ion source temperature was 300°C.

Purification of cpd1335. A cell surface extract from a 250-ml culture of strain RSpMarA2 was collected using the previously described method. During concentration under reduced pressure, a 1,335-Da compound (cpd1335) precipitated. The precipitate was washed three times with deionized water, resulting in crude, desalted cpd1335. Pure cpd1335 was obtained using reverse-phase (RP) HPLC (Grom-Sil ODS-5 ST column, 20 by 250 mm; Alltech-Grom, Rottenburg-Hailfingen, Germany) with a linear gradient elution of 40 to 70% aqueous acetonitrile with 0.1% (vol/vol) formic acid over 40 min at a flow rate of 15 ml/min.

MALDI-TOF mass spectrometric analysis. Strains were grown for 16 h at 37°C on production media solidified with 1.5% agar. For preparation of surface extracts, colonies were picked from the agar plates and extracted by vortexing for 30 s with 50 μ l 70% acetonitrile–30% water with 0.1% formic acid. Matrix-assisted laser desorption/ionization–time of flight (MALDI-TOF) mass spectra were recorded using a Bruker Autoflex MALDI-TOF instrument containing a 337-nm nitrogen laser for desorption and ionization. Samples (2 μ l) were mixed with the same volume of matrix solution (a saturated solution of α -cyano-4-hydroxycinnamic acid in 50% aqueous acetonitrile containing 0.1% [vol/vol] trifluoroacetic acid), spotted on the target, air dried, and measured as described previously (36). Spectra were obtained by positive ion detection and reflector mode MS.

RT-PCR. Total RNA was isolated with the Qiagen RNeasy minikit. Cells (OD_{600} , 1.0) were harvested from M9 minimal medium supplemented with BME

vitamin mix (catalog no. B6891) and ATCC trace mineral solution (catalog no. MD-TMS) and treated with the Qiagen RNeasy protect bacterial reagent. Harvested cells were resuspended in 250 μ l of 10 mM Tris (pH 8.5) with 15 mg/ml lysozyme and 5 μ l proteinase K (20 mg/ml) and digested for 1 h at 22°C with gentle agitation. A DNase I digestion was performed for *pznE* and *pznL* using the Qiagen RNase-free DNase set. DNase I (7 μ l) and Qiagen RDD DNA digest buffer (7 μ l) were used to hydrolyze contaminating DNA for 20 min at 22°C. The RNA isolation protocol was then performed according to the manufacturer's instructions. To minimize background, a DNase I digestion (5 μ l) was executed with the RNA samples and placed at 37°C for 20 min. Note that this was the second DNase I digest for *pznE* and *pznL*. Samples were column purified using the RNA cleanup protocol in the RNeasy minikit handbook (Qiagen). Digestion and cleanup were repeated for all RNA samples, excluding those used to analyze *pznE* and *pznL*. cDNA was prepared with commercially available reverse transcriptase PCR (RT-PCR) kits using 1 μ g of RNA and the primers listed in Table 2.

Tris-Tricine-SDS-PAGE. Gels (18%) were prepared according to Schägger and von Jagow (32), with water instead of glycerol and without a spacer gel. Cellular extracts (100 μ l) were mixed with 5 \times SDS sample buffer (20 μ l) and then heated at 100°C for 5 min prior to gel loading, along with an ultra-low-range molecular weight marker (Sigma). The peptides were separated by low-current (30-mA) electrophoresis. The gel was subsequently washed with destaining solution (10 ml ethanol, 10 ml acetic acid, 50 ml water) for 20 min (three times) and in deionized water for 20 min (three times). The gel was stained with Coomassie EZBlue (Sigma) and/or Schiff's reagent (Sigma) after 1 h of oxidation with 0.7% (vol/vol) periodic acid. The Coomassie EZBlue-stained band was excised from the gel and extracted with 50 μ l 70% acetonitrile–30% water with 0.1% (vol/vol) formic acid for 24 h. The supernatant was used for MALDI-TOF MS measurement.

RESULTS

MALDI-TOF MS detection of a new metabolite from FZB42 with $[M + H]^+$ 1,336 Da. *B. amyloliquefaciens* FZB42 is a prolific producer of antibacterial and antifungal natural products. To date, nonribosomally produced peptides, including three antimicrobial lipopeptides (surfactin, bacillomycin D, and fengycin), three polyketide antibiotics (bacillaene, difficidin, and macrolactin), the antibacterial dipeptide bacilysin, and two siderophores (bacillibactin and the putative product of the *nrs* gene cluster) have been identified (7). In addition to the discovery of these compounds, small-molecule metabolite screening of FZB42 by MALDI-TOF MS revealed a metabolite with a molecular mass $[M + H]^+$ of 1,336 Da (Fig. 2A, cpd1335). The visible species at m/z 1,354 Da indicates that this compound also appears in a hydrated form (Fig. 2A) (+18 Da). This may be attributed to a hydrolysis product, given that

TABLE 3. Activity spectrum of plantazolicin

Indicator strain	Degree of inhibition ^a	Source or reference ^b
<i>Bacillus brevis</i> ATCC 8246	+	ATCC
<i>Bacillus subtilis</i> 168	+	4
<i>Bacillus cereus</i> ATCC 14579	+	ATCC
<i>Bacillus licheniformis</i> ATCC 9789	+	ATCC
<i>Micrococcus luteus</i>	+	Laboratory collection
<i>Bacillus pumilus</i>	–	Laboratory collection
<i>Bacillus subtilis</i> CU1065	+	4
<i>Bacillus subtilis</i> HB0042	++	4
<i>Bacillus sphaericus</i>	+	Laboratory collection
<i>Paenibacillus polymyxa</i>	–	Laboratory collection
<i>Paenibacillus granivorans</i>	+	Laboratory collection
<i>Bacillus megaterium</i> 7A1	++	Laboratory collection
<i>Arthrobacter</i> sp.	–	Laboratory collection
<i>Staphylococcus aureus</i>	–	Laboratory collection
<i>E. coli</i> K-12	–	Laboratory collection
<i>Klebsiella terrigena</i>	–	Laboratory collection
<i>Pseudomonas</i> sp.	–	Laboratory collection
<i>Erwinia carotovora</i>	–	Laboratory collection

^a ++, inhibition; +, weak inhibition; –, no inhibition.

^b ATCC, American Type Culture Collection.

the +18-Da signal progressively dominates after extensive sample manipulation (data not shown). As with the lipopeptide products, mass spectrometric signals from this compound were detected in surface extracts and in the culture filtrate. Based on our previous work on small-molecule metabolites from FZB42 (6), we surmise that after biosynthesis, cpd1335 is actively transported out of the cell. After export, the product presumably accumulates in the peptidoglycan layer of FZB42, with a portion being spontaneously released into the culture medium. Thus, we set out to determine the biosynthetic origin of cpd1335.

Previously, we generated a strain of FZB42, dubbed RS6, that is deficient in the production of all Sfp-dependent lipopeptides and polyketides and the Sfp-independent synthesis of bacilysin (*sfp::ermAM bac::cm*) (Table 1) (9). We were initially surprised when strain RS6 was still capable of producing cpd1335, as assessed by MALDI-TOF MS (Fig. 2B). Clearly, this natural product is not being assembled by typical nonribosomal machinery, such as the nonribosomal peptide synthetase (NRPS) and polyketide synthase (PKS) biosynthetic pathways. This suggested either that FZB42 was assembling cpd1335 using an unrecognized Sfp or that cpd1335 was of ribosomal origin (i.e., a bacteriocin). Despite the absence of all known nonribosomally synthesized secondary metabolites (9), supernatants of the RS6 mutant strain retained antagonistic activity toward closely related *Bacilli*, such as *Bacillus megaterium*, *B. subtilis* 168 (*trpC2*), and a *sigW* mutant of *B. subtilis* designated strain HB0042 (Table 3). Butcher and Helmann have reported that the growth of *B. subtilis* HB0042 was inhibited by an unknown substance, a potential bacteriocin, produced by FZB42 (4). Further, BLAST searching returns only one copy of Sfp in the FZB42 genome (1). These findings led us to favor the hypothesis that cpd1335 was a ribosomally synthesized antibacterial substance, which heretofore has not been reported in FZB42.

Preliminary characterization of cpd1335. The nonconcentrated, cell surface extract of RSpMarA2, the strain which

bears a *mariner* transposon insertion in the *degU* global transcriptional regulator gene (20), contains significantly higher levels of cpd1335 than those in the wild type and the RS6 mutant strain (Table 1; Fig. 3A). Due to the elevated production level of cpd1335, strain RSpMarA2 was employed for further characterization. The dialyzed surface extract of RSpMarA2 was separated by Tris-Tricine-SDS-PAGE and stained with Coomassie EZBlue (Fig. 4A). While the Coomassie EZBlue stain was relatively weak, we were able to achieve an improved visualization of the peptide-sized band (1 to 2 kDa) by double staining with Schiff's reagent after oxidation with periodic acid (Fig. 4B). Periodic acid oxidizes alcohols to aldehydes, which then react with Schiff's reagent (15). The band, which presumably contained cpd1335, based on electrophoretic migration, was excised for further characterization. After extraction from the gel, MALDI-TOF MS identified *m/z* 1,354 Da as the most intense ion in the monitored mass window (Fig. 4C), corresponding to the hydrated form $[M + H_2O + H]^+$ of cpd1335. Given that this apparent hydrated product was detected earlier (Fig. 2), it was not surprising that after extensive sample preparation (gel electrophoresis and extraction), the hydrated product was the major species. Cpd1335 was found to be growth inhibitory toward closely related Gram-positive *Bacilli*, but no activity was observed toward Gram-negative bacteria, such as *Erwinia carotovora*, *Escherichia coli* K-12, *Klebsiella terrigena*, and *Pseudomonas* sp. (Table 3).

Solubility profiling of purified cpd1335 revealed that this natural product is extractable with chloroform, separable by reverse-phase HPLC, and insoluble in water at high concentrations (Fig. 3). Taken together, our solubility data and production from strain RS6 suggest that cpd1335 is a relatively hydrophobic, extensively modified peptide of ribosomal origin.

Bioinformatic assessment of the cpd1335 biosynthetic genes. Supported by the above preliminary characterization of cpd1335, we performed a literature search for small, hydrophobic, modified, antibacterial peptides produced by Gram-positive bacteria. Research on thiopeptides revealed characteristics similar to those of cpd1335 (18, 25, 27, 39). Interestingly, several orthologs to the genes involved in thiopeptide biosynthesis can be found clustered in FZB42, suggesting that cpd1335 may be synthesized by a related route. Introduction of a spectinomycin antibiotic cassette within one of these orthologous genes (RBAM_007480, a putative flavin mononucleotide-dependent dehydrogenase) resulted in mutant RS26, which was unable to produce cpd1335, as assessed by mass spectrometry (Fig. 3A). This result strongly suggested that cpd1335 was a thiazole/oxazole-modified microcin (TOMM).

In addition to indicating similarity to proteins involved in thiopeptide biosynthesis, protein BLAST (1) and ClustalW (34) sequence alignment have demonstrated that the FZB42 TOMM biosynthetic proteins also exhibit modest similarity to a previously characterized cytolytic TOMM from *Streptococcus pyogenes* (23). The TOMM biosynthetic locus from *S. pyogenes* is referred to as the *sag* cluster, for SLS-associated genes. SagB (dehydrogenase), SagC (cyclodehydratase), and SagD (docking protein) are homologous to RBAM_007480 (20% identical, 53% similar), RBAM_007460 (13% identical, 50% similar), and RBAM_007470 (19% identical, 58% similar),

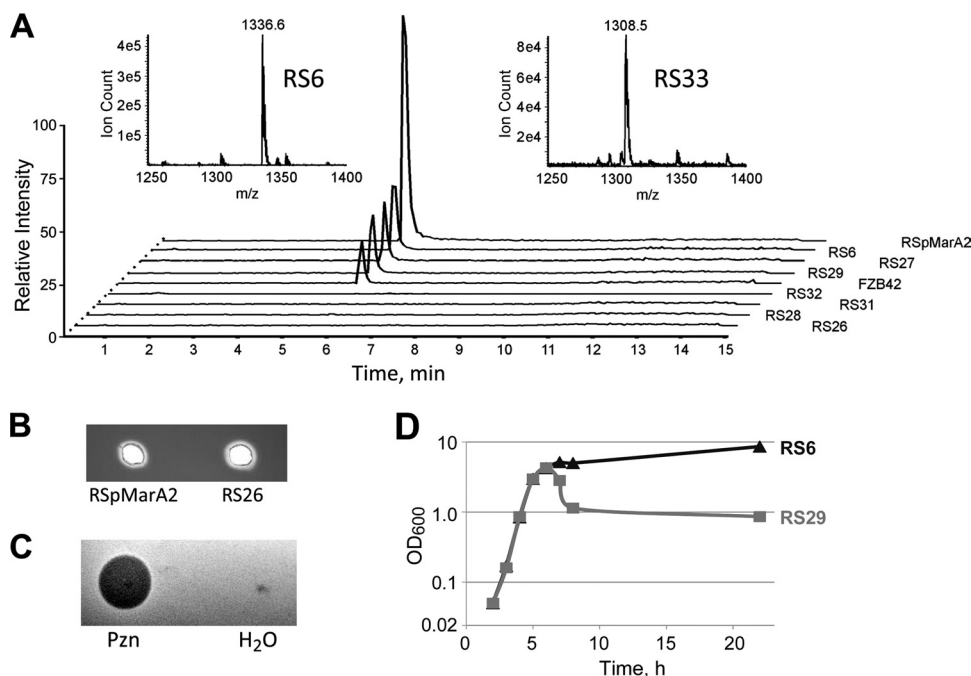


FIG. 3. Effect of mutations in the *pzn* gene cluster on biological activity. (A) Extracted ion chromatogram of PZN ($[M + H]^+$ 1,336 Da) of FZB42 and mutant strains. This compound (m/z 1,336.6 Da) (left inset) is synthesized by wild-type FZB42 and by the mutant strains RS6 ($\Delta sfp \Delta bac$), RS27, and RS29. RSpMarA2 ($\Delta degU$) overproduces PZN. Strains RS26, RS28, RS31, and RS32 were deficient in PZN production. Strain RS33 (right inset) produced a compound with m/z 1,308.5 Da, suggesting the loss of two methyl groups ($-H_2 + C_2H_6$, -28 Da). (B) Hemolytic activity of 100 μ l extract from RSpMarA2 and RS26 on blood agar plates. (C) Antibacterial activity of PZN. (Left) HPLC-purified PZN (10 μ l of 100 μ g/ μ l suspended in water) was spotted onto an agar plate of *B. subtilis* HB0042 (*sigW* null) and incubated for 16 h to assess growth inhibition. (Right) Water (10 μ l; negative control). (D) Growth curves of strains RS6 and *pznF* mutant RS29. After approximately 20 h of growth, the RS29 culture density is 9 log units lower than that of RS6.

respectively. Also bearing similarity to the SLS biosynthetic cluster are RBAM_007490 (SagE, Caax protease; 16% identical, 54% similar), RBAM_007420 (SagG, ABC transporter; 15% identical, 53% similar), and RBAM_007430 (SagH, ABC transporter; 22% identical, 63% similar) (12, 23). Due to this similarity, we have adopted the *sag* lettering nomenclature for this biosynthetic cluster (Fig. 5). Despite the genetic similarities between SLS and cpd1335, there is no difference in the hemolytic activities of RSpMarA2 (cpd1335 overproducer)

and mutant RS26 (devoid of cpd1335 production) on blood agar plates containing the concentrated, dialyzed cell surface extract (Fig. 3B). This demonstrates that cpd1335 is not required for the hemolytic activity of FZB42 and suggests that cpd1335 exhibits other biological activity.

Preliminary biological activity for cpd1335. It is important to note that although there is remarkable similarity in the genetic organizations of the TOMM biosynthetic clusters, the chemical structures and biological targets of the resultant nat-

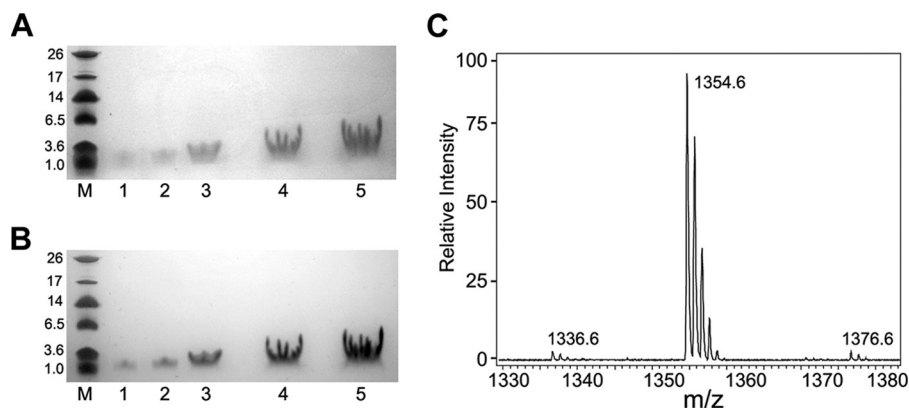


FIG. 4. Characterization of cell surface extract. Samples were prepared from RSpMarA2 and separated by 18% Tris-Tricine-SDS-PAGE either stained with Coomassie EZBlue (A) or double-stained with Coomassie EZBlue and Schiff's reagent (B). Lane M, molecular size markers; lanes 1 to 5, 1 μ l, 2 μ l, 5 μ l, 10 μ l, and 20 μ l surface extract. (C) MALDI-TOF mass spectrum of the hydrated form of PZN (m/z 1,336 + 18 = 1,354 Da) obtained by excising the peptide band from the Tris-Tricine-SDS-PAGE gel.

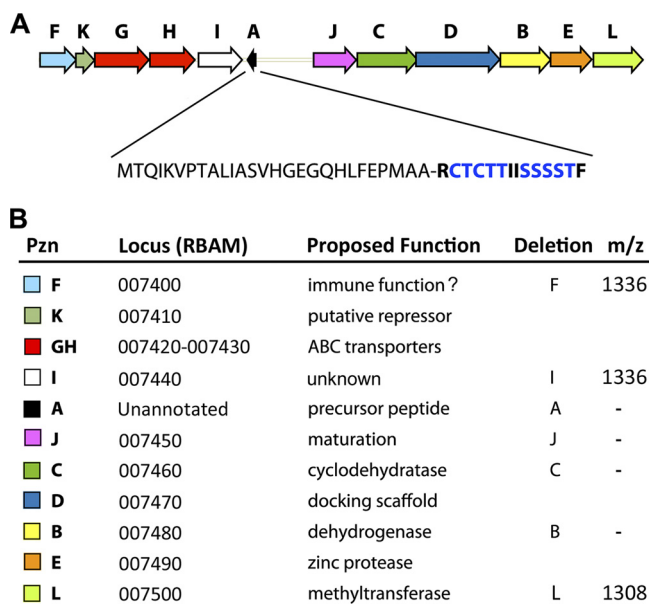


FIG. 5. Plantazolicin gene cluster. (A) FZB42 PZN gene cluster (9,892 bp) and amino acid sequence of the precursor peptide. -, putative leader peptide processing site. (B) Proposed functions of individual PZN genes. Upon deletion of *pznF* and *pznI*, cpd1335 (PZN) was detected by mass spectrometry. Deletion of *pznL* resulted in desmethyl PZN (*m/z* 1,308 Da), while individual inactivation of all other tested genes (*pznABCJ*) did not produce PZN. The functions of *pznF*, *pznI*, and *pznJ* require further exploration, but preliminary data suggest that *pznF* plays a role in immunity, *pznI* encodes a pentapeptide repeat protein, and *pznJ* is required for PZN maturation.

ural products vary widely (e.g., SLS, cellular membrane; microcin B17, DNA gyrase; thiostrepton/thiocillin, 50S ribosome; and cyanobactins, anticancer activity). Previous data have shown that the specific biological activity of the TOMM product is encoded by the sequence of the precursor peptide and that the cyclodehydratase, dehydrogenase, and docking protein are functionally redundant (23). Although this study has not elucidated the molecular target of cpd1335, we have deter-

mined that the purified compound is growth inhibitory toward most of the Gram-positive *Bacilli* surveyed, especially *B. megaterium* and *B. subtilis* HB0042 (Fig. 3C; Table 3). Interestingly, extracts of mutant RS26, which do not contain cpd1335, were still capable of suppressing the growth of *B. subtilis* HB0042. This shows that cpd1335 was not solely responsible for the specific antibiotic activity previously observed in FZB42 culture fluid (4). These results demonstrate that FZB42 biosynthesizes at least one additional narrow-spectrum antibiotic, which like cpd1335 is likely synthesized by ribosomes.

As demonstrated by our mass spectrometry studies (Fig. 2), cpd1335 requires a TOMM-type dehydrogenase for production (Fig. 1, 5). RBAM_007480 is a *sagB*-like gene, embedded within a cluster of 12 genes involved in the biosynthesis, export, and immunity of a posttranslationally modified, hydrophobic natural product (Fig. 5). The defining feature of all TOMM natural products is the incorporation of Cys- and Ser/Thr-derived heterocycles onto a ribosomally synthesized, peptidic backbone. To highlight these suspected modifications, we herein refer to cpd1335 as plantazolicin (PZN). The PZN biosynthetic 12-gene cluster spans nearly 10 kb of the FZB42 chromosome (Fig. 5). As in SLS and microcin B17 production, a trimeric thiazole/oxazole BCD synthetase complex is present. Based on their similarity to these systems, all three genes (*pznBCD*) are required for heterocycle formation (*pznC*, RBAM_007460; *pznD*, RBAM_007470) (Fig. 5).

RT-PCR. Transcription of all 12 *pzn* genes in M9 minimal media was confirmed by reverse transcriptase PCR (RT-PCR) (Fig. 6). All amplicons migrated with their expected sizes (Table 2). In addition to confirming transcription, we also assessed the intergenic regions of the PZN biosynthetic cluster to determine if the mRNA was polycistronic. Using the appropriate primers from adjacent genes, we determined that the biosynthetic genes are transcribed into two polycistronic mRNAs (*pznFKGHI* and *pznJCDBEL*) and a monocistronic mRNA for *pznA* (Fig. 6). Amplification of the region between *pznE* and *pznL* resulted in a band that was visible only under extreme contrast (data not shown). Numerous attempts to amplify the *pznIJ* junction were unsuccessful.

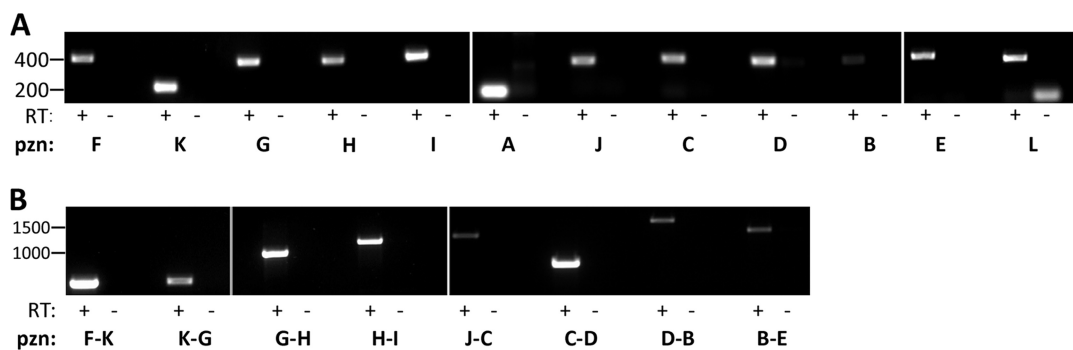


FIG. 6. RT-PCR reveals polycistronic mRNAs. Reverse transcriptase (RT) PCR was performed using 1 μ g of FZB42 RNA isolated from stationary phase using a commercially available kit. PCR products were analyzed in comparison to a negative control lacking reverse transcriptase (-RT). (A) All genes in the putative PZN cluster are transcribed under the culturing conditions employed. Cells (1 ml at an OD_{600} of 1.0) were removed from a stationary culture growing at 37°C 24 h after inoculation. Total RNA was isolated and converted to cDNA by RT-PCR. cDNA (500 ng), excluding *pznE* and *pznL* (750 ng each), was added to each reaction mixture. Gene fragments were then amplified using specific primers and PCR. Amplicons were assessed by separation on 1.1% agarose gels containing ethidium bromide and visualized by UV illumination. (B) Amplification of adjacent *pzn* genes reveals polycistronic mRNA. Junction I-J did not reveal a significant band; junction E-L was visible under extreme contrast (data not shown). All amplicons migrate on the basis of their expected sizes. Numbers at left represent DNA size standards.

Functional analysis of the *pzn* gene cluster by gene-targeted mutagenesis. (i) **Precursor peptide gene.** As with many TOMM clusters, the gene encoding the precursor peptide is not annotated as an open reading frame (ORF) in the FZB42 genome (GenBank accession no. CP000560.1) (23). This gene was identified by a manual ORF search and found to be encoded between *pznI* (RBAM_007440) and *pznJ* (RBAM_007450) in the opposite direction. Although unannotated, this ORF (*pznA*) bears a robust Shine-Dalgarno sequence, AGGAGG, which is found 8 bp upstream of an AUG start codon. *pznA* is predicted to encode only 41 amino acids (Fig. 5A), which is 6 shorter than previously reported (23). The C-terminal region, also known as the core peptide (28), is rich in residues that can be enzymatically cyclized to thiazoles and (methyl)oxazoles (2 Cys, 4 Thr, and 4 Ser residues). This feature is a clear indicator of TOMM precursor peptides (14, 23, 39) (Fig. 1). As expected, the *pznA* mutant RS32 was also deficient in synthesis of PZN (Fig. 3A and 5).

(ii) **Operon structure and transcriptional regulation.** The *pzn* biosynthetic gene cluster is partitioned into three sections. The first operon (*pznFKGHI*) consists of genes predicted to be involved in immunity, regulation, and transport (Fig. 5). The product of *pznK* (RBAM_007410) is related to homodimeric repressor proteins of the ArsR family (3). This protein possibly regulates the expression of other *pzn* genes through an unexplored mechanism. The second operon (*pznJCDBEL*) harbors the genes encoding the enzymes responsible for converting the inactive PznA precursor peptide into the mature, bioactive natural product. The third section of the biosynthetic cluster contains only the *pznA* gene. This gene encodes the precursor peptide and faces in the opposite direction relative to all other *pzn* genes. A summary of the putative functions of the members of the *pzn* gene cluster in *B. amyloliquefaciens* FZB42 is given in Fig. 5B.

(iii) **Enzymatic processing of PznA.** The enzymes dedicated to the modification and processing of the PznA precursor peptide are encoded by the second operon of the PZN biosynthetic cluster (*pznJCDBEL*) (Fig. 5). The function of the first gene, *pznJ*, is not known; however, uncharacterized orthologs can also be found in two plant-associated, Gram-positive organisms, *Bacillus pumilus* and *Clavibacter michiganensis*. For the latter organism, *pznJ* is annotated as a putative hydroxylase. Sequence analysis and literature searching fail to substantiate this designation. As with the creation of other mutant strains, we applied the SOE method (16) to replace *pznJ* with a spectinomycin resistance gene. The resulting mutant, RS28, did not produce PZN (Fig. 3A and 5), demonstrating that PznJ plays a vital biosynthetic role.

Based on sequence alignment, PznC is related to the TOMM cyclodehydratase present in *S. pyogenes*, SagC. Previous research on SagC revealed its importance in substrate (SagA) recognition, in addition to its ability to catalyze the peptide backbone cyclization of Cys, Ser, and Thr residues (26). Based on this information, we generated a mutant interrupted in *pznC*, RS31 (Table 1). As expected, this mutant does not produce PZN (Fig. 3A). We did not prepare a deletion mutant of *pznD* (RBAM_007470) or *pznE* (RBAM_007490). PznD is highly similar to SagD from the SLS biosynthetic cluster and is termed the docking scaffold protein. According to previous studies (23), the docking protein appears to be

involved in “BCD” trimer formation and regulation of enzymatic activity. Therefore, PznD is expected to be of significant importance in the maturation process of PznA. PznE belongs to the type II CaaX protease family (29). As predicted by OCTOPUS (38), PznE contains 4 transmembrane domains, as do the type II CaaX proteases from *S. pyogenes*, *Clostridium botulinum*, *Staphylococcus aureus*, and *Listeria monocytogenes* (23). We hypothesize that this protein will function as a leader peptidase, proteolytically processing the PznA peptide at PMAA/R (Fig. 5A). Two arguments supporting this site as the putative leader peptide processing site are that (i) cleavage between or before the Ala residues is unlikely, given the molecular mass of the resultant peptide and the number of modifiable residues, and (ii) bacteriocin leader peptides are most often processed after a Gly-Gly sequence, but other small residues, such as Ser and Ala, can be found directly N terminal to the scissile bond (13, 28, 35).

The product of the last gene within the cluster, PznL (RBAM_007500), was identified by sequence analysis to be an S-adenosylmethionine (SAM)-dependent methyltransferase (Fig. 5). Mutant RS33, devoid of *pznL* (Table 1), produced a compound with *m/z* 1,308.5 Da, indicating a loss of 28 Da relative to the mass of the wild type. Based on this data, PznL is responsible for the transfer of two methyl groups to PZN [$\text{CH}_3 = 15 \text{ Da}; (2 \times 15) - 2\text{H} = 28 \text{ Da}$] (Fig. 3A, right inset).

(iv) **Natural product export and immunity.** As mentioned above, *pznG* (RBAM_007420) and *pznH* (RBAM_007430) are homologous to ABC transporters, with PznG being responsible for binding ATP and PznH carrying out the permease activity. ABC transporters are common constituents of TOMM biosynthetic gene clusters and are present across many taxa of bacteria and archaea (23). The functions of the *pznF* (RBAM_007400) and *pznI* (RBAM_007440) gene products are more convoluted. It has previously been hypothesized that one or both of these gene products could be involved in the self-immunity of FZB42 against PZN (23). While a protein BLAST database search on PznF yields homology to putative membrane proteins, PznI is annotated as a pentapeptide repeat protein. Research on other proteins of the pentapeptide repeat family has revealed that they play important signaling roles via coordinating protein-protein interactions (37) and can also confer resistance to quinolone antibiotics (30). To address their potential role in PZN production/immunity, the *pznI* and *pznF* genes were individually replaced with the spectinomycin resistance gene. Although both of these mutants were still able to produce PZN (Fig. 3A), they displayed different growth characteristics. Neither mutant exhibited visible growth defects during growth on LB agar plates. In liquid LB media, the *pznI* mutant (RS27) growth curve was indistinguishable from that of the background strain (RS6). However, the *pznF* mutant (RS29) displayed markedly different growth behavior. Upon reaching a maximum culture density, which was equal to that of RS6, RS29 appeared to undergo lysis instead of maintaining a high culture density (Fig. 3D). Mature PZN is present in a quantity sufficient to be detected by MALDI mass spectrometry during the early stationary growth phase (Fig. 2) but not at earlier time points (data not shown). This suggests that the *pznF* mutant is more susceptible to the actions of an antimicrobial compound produced in higher abundance during later growth phases. Upon treating RS6 and RS29 with purified

PZN, a larger zone of inhibition was visible for the RS29 strain, confirming that the above-described growth phenotype was indeed PZN dependent (data not shown). Given the observation that FZB42 requires an immunity gene (*pznF*) for fully competent growth and that PZN exhibits activity against only select Gram-positive bacteria (Table 3), we conclude that PZN acts as a narrow-spectrum antibacterial compound.

DISCUSSION

A novel, antibacterial, microcin B17/streptolysin-like compound with a molecular mass $[M + H]^+$ of 1,336 Da (plantazolicin [PZN]) was identified in the culture supernatant and cell surface extract from *B. amyloliquefaciens* FZB42. We postulate that the core peptide consists of 14 amino acids (RCTCTTISSSTF), 10 of which potentially serve as a site of heterocycle formation (Cys, Ser/Thr). Although we have not yet ascertained the precise chemical structure of PZN, supportive evidence that demonstrates that this natural product undergoes extensive posttranslational modification is available (Fig. 2 to 4). Numerous attempts to elucidate the structure of PZN by liquid chromatography (LC) ESI-MS/MS (tandem) analysis showed an unusually incomplete fragmentation pattern (data not shown). Such tandem MS analysis (i.e., collision-induced dissociation) tends to fragment parent ions at the amide bond, leading to a series of ions containing the N terminus (b-ion series) and the C terminus (y-ion series). If contiguous heterocycles were indeed formed on adjacent residues of PznA, an incomplete tandem spectrum would be the expected outcome. A full structural elucidation of PZN by other spectroscopic methods is under way and will be the subject of a future publication.

A previous bioinformatics survey revealed modest similarity of a putative biosynthetic locus from FZB42 with the streptolysin S (SLS) biosynthetic operon from *Streptococcus pyogenes* (23). Genes from this operon are designated SLS-associated genes (*sag*), of which there are a total of 9 (*sagA* to *-I*). Related gene clusters have been widely disseminated among bacteria and archaea. The genetic and biochemical conservation within this particular natural product family has led to a new classification of small, highly modified bacteriocins, the thiazole/oxazole-modified microcins (TOMMs) (14, 23). Genetic ablation of RBAM_007480, a gene homologous to *sagB*, resulted in the inability of FZB42 to synthesize PZN (Fig. 3). Thus, the FZB42 TOMM cluster appeared to be responsible for the synthesis of PZN. Analysis of the local genomic context of RBAM_007480 identified a 12-gene biosynthetic cluster encoding hypothetical genes involved in TOMM biosynthesis, immunity, and export (Fig. 5). The TOMM precursor gene, *pznA*, encodes a small peptide consisting of 41 amino acids. Like *pznB* (the *sagB* ortholog), deletion of *pznA*, among other essential genes (e.g., *pznC*), abolishes the production of PZN. After PznBCD-dependent heterocycle formation, dimethylation (PznL), and N-terminal processing by a protease (possibly PznE), the core peptide of modified PznA is secreted into the exterior environment via the ABC transporters PznG and PznH. In addition to establishing the order and location of all posttranslational events, we are investigating the biosynthetic role of the requisite PznJ protein in our laboratory.

Several gene clusters encoding TOMMs have been detected

in the genomes of plant-associated bacteria, such as *Bradyrhizobium japonicum*, *Pseudomonas putida*, and *Clavibacter michiganensis* (23). Performing a protein BLAST search using each *pzn* gene product as the query sequence returns orthologous protein matches from *Bacillus pumilus* ATCC 7061 as the top hit after FZB42 itself. The thiazole/oxazole synthetase proteins (PznBCD) from *B. pumilus* (protein identifiers EDW22765.1, EDW22903.1, and EDW23125.1, respectively) demonstrated a remarkable degree of amino acid identity to those from FZB42 (PznB, 77%; PznC, 63%; and PznD, 82%). Moreover, the *pzn* genes from *B. pumilus* are found clustered and in an order identical to that found in FZB42. Also like FZB42, *B. pumilus* is a plant saprophyte that produces an array of antibacterial and antifungal natural products (10). Further, the PznA core peptide sequences from FZB42 and *B. pumilus* (unannotated, located between EDW23486.1 and EDW22932.1) are 100% identical. Considering all of these factors, we predict that *B. pumilus* is also a PZN producer.

Interestingly, the *pzn* gene cluster was absent from the genome of *B. amyloliquefaciens* type strain DSM7^T (EMBL identifier FN597644), a non-plant-associated bacterium. It is plausible that the *pzn* gene cluster in FZB42 has been horizontally transferred between members of the plant rhizosphere. To bolster this possibility, we performed a protein BLAST search of three draft genomes of plant-associated *B. amyloliquefaciens* strains, which recently became available (2). Within the *B. amyloliquefaciens* CAU-B946 genome, we found the complete 12-gene PZN biosynthetic cluster, displaying 95 to 100% amino acid identity with that of FZB42. The genomes of strains *B. amyloliquefaciens* YAU-Y2 and NAU-B3 did not possess the complete set of genes for the PZN cluster but did harbor a portion of the immunity/transport operon, *pznFKGH*. These genes displayed 95 to 100% identity with the corresponding genes from FZB42. Although the YAU-Y2 and NAU-B3 genomes lack an intact PZN biosynthetic cluster, the genetic compositions of these strains imply that the plant-associated members of the *B. amyloliquefaciens* (plantarum) taxon are at least immune toward, and/or capable of, the *de novo* synthesis of PZN.

A detailed biological function for PZN has yet to be established. Unlike with some TOMMs, a functional prediction cannot reliably be made based on the sequence of *pznA* due to its lack of homology to other TOMM precursors with known functions. In other words, TOMM precursor peptides similar in sequence to *SagA* are cytolysins (11, 26), while unrelated sequences do not encode cytolytic activity (i.e., the precursors for microcin B17, patellamides, thiostrepton, etc.). Our preliminary results demonstrate that PZN functions as a narrow-spectrum antibacterial compound. Presumably, this natural product is meant to suppress the growth of taxonomically related competitors within the plant rhizosphere. Independent of function, PZN should be highly protected from degradation by peptidases within the plant rhizosphere, due to an extensive degree of modification.

ACKNOWLEDGMENTS

The strains CU1065 and HB0042 were kindly provided by J. Helmann (Cornell University, Ithaca, NY). *B. amyloliquefaciens* strains CAU-B946, YAU-Y2, and NAU-B3 were obtained from Q. Wang (Chinese Agricultural University, Beijing, China), Y. He (Yunnan

Agricultural University, Kunming, China), and X. Gao (Nanjing Agricultural University, Nanjing, China), respectively. We are very grateful to A. Pühler, C. Rückert, and J. Blom (CeBiTec, Bielefeld University, Bielefeld, Germany) for support in the draft genome sequencing of the above-mentioned strains. We are indebted to D. Naumann, P. Lasch (Robert Koch-Institut Berlin), and J. Melby (University of Illinois) for assistance with mass spectrometry. Members of the Mitchell lab are acknowledged for critical review of the manuscript.

The work was supported by funds of the competence network Genome Research on Bacteria (GenoMikPlus), the Chinese-German collaboration project 0330798A, financed by the German Ministry for Education and Research (R.B.), the Cluster of Excellence program Unifying Concepts in Catalysis, coordinated by the Technische Universität Berlin (R.S.), Ruth L. Kirschstein National Research Service Award NIH/NCI T32 CA009523 (A.L.M.), and institutional funds provided by the University of Illinois (D.A.M.).

REFERENCES

- Altschul, S. F., T. L. Madden, A. A. Schaffer, J. Zhang, Z. Zhang, W. Miller, and D. J. Lipman. 1997. Gapped BLAST and PSI-BLAST: a new generation of protein database search programs. *Nucleic Acids Res.* **25**:3389–3402.
- Borriss, R., X. Chen, C. Rueckert, J. Blom, A. Becker, B. Baumgarth, B. Fan, R. Pukall, P. Schumann, C. Sproer, H. Junge, J. Vater, A. Puhler, and H. P. Klenk. 3 September 2010. Relationship of *Bacillus amyloliquefaciens* clades associated with strains DSM7T and FZB42: a proposal for *Bacillus amyloliquefaciens* subsp. *amyloliquefaciens* subsp. nov. and *Bacillus amyloliquefaciens* subsp. *plantarum* subsp. nov. based on their discriminating complete genome sequences. *Int. J. Syst. Evol. Microbiol.* [Epub ahead of print.] doi:10.1099/ijs.0.023267-0.
- Busenlehner, L. S., M. A. Pennella, and D. P. Giedroc. 2003. The SmtB/ArsR family of metalloregulatory transcriptional repressors: structural insights into prokaryotic metal resistance. *FEMS Microbiol. Rev.* **27**:131–143.
- Butcher, B. G., and J. D. Helmann. 2006. Identification of *Bacillus subtilis* sigma-dependent genes that provide intrinsic resistance to antimicrobial compounds produced by Bacilli. *Mol. Microbiol.* **60**:765–782.
- Chen, X. 2009. Whole genome analysis of the plant growth-promoting rhizobacteria *Bacillus amyloliquefaciens* FZB42 with focus on its secondary metabolites. Ph.D. dissertation. Humboldt-Universität zu Berlin, Berlin, Germany.
- Chen, X.-H., A. Koumoutsis, R. Scholz, and R. Borriss. 2009. More than anticipated-production of antibiotics and other secondary metabolites by *Bacillus amyloliquefaciens* FZB42. *J. Mol. Microbiol. Biotechnol.* **16**:14–24.
- Chen, X.-H., A. Koumoutsis, R. Scholz, A. Eisenreich, K. Schneider, I. Heinemeyer, B. Morgenstern, B. Voss, W. R. Hess, O. Reva, H. Junge, B. Voigt, P. R. Jungblut, J. Vater, R. Süßmuth, H. Liesegang, A. Strittmatter, G. Gottschalk, and R. Borriss. 2007. Comparative analysis of the complete genome sequence of the plant growth-promoting bacterium *Bacillus amyloliquefaciens* FZB42. *Nat. Biotechnol.* **25**:1007–1014.
- Chen, X.-H., A. Koumoutsis, R. Scholz, K. Schneider, J. Vater, R. Süßmuth, J. Piel, and R. Borriss. 2009. Genome analysis of *Bacillus amyloliquefaciens* FZB42 reveals its potential for biocontrol of plant pathogens. *J. Biotechnol.* **140**:27–37.
- Chen, X.-H., R. Scholz, M. Borriss, H. Junge, G. Mogel, S. Kunz, and R. Borriss. 2009. Difficidin and bacillisin produced by plant-associated *Bacillus amyloliquefaciens* are efficient in controlling fire blight disease. *J. Biotechnol.* **140**:38–44.
- Choudhary, D. K., and B. N. Johri. 2009. Interactions of *Bacillus* spp. and plants—with special reference to induced systemic resistance (ISR). *Microbiol. Res.* **164**:493–513.
- Cotter, P. D., L. A. Draper, E. M. Lawton, K. M. Daly, D. S. Groeger, P. G. Casey, R. P. Ross, and C. Hill. 2008. Listeriolysin S, a novel peptide haemolysin associated with a subset of lineage I *Listeria monocytogenes*. *PLoS Pathog.* **4**:e1000144.
- Datta, V., S. M. Myskowski, L. A. Kwinn, D. N. Chiem, N. Varki, R. G. Kansal, M. Koth, and V. Nizet. 2005. Mutational analysis of the group A streptococcal operon encoding streptolysin S and its virulence role in invasive infection. *Mol. Microbiol.* **56**:681–695.
- Dirix, G., P. Monsieurs, K. Marchal, J. Vanderleyden, and J. Michiels. 2004. Screening genomes of Gram-positive bacteria for double-glycine-motif-containing peptides. *Microbiology* **150**:1121–1126.
- Haft, D. H., M. K. Basu, and D. A. Mitchell. 2010. Expansion of ribosomally produced natural products: a nitrile hydratase- and Nif11-related precursor family. *BMC Biol.* **8**:70.
- Hardonk, M. J., and D. Van. 1964. The mechanism of the Schiff reaction as studied with histochemical model systems. *J. Histochem. Cytochem.* **12**:748–751.
- Horton, R. M., Z. L. Cai, S. N. Ho, and L. R. Pease. 1990. Gene splicing by overlap extension: tailor-made genes using the polymerase chain reaction. *Biotechniques* **8**:528–535.
- Idriss, E. E., O. Makarewicz, A. Farouk, K. Rosner, R. Greiner, H. Bochow, T. Richter, and R. Borriss. 2002. Extracellular phytase activity of *Bacillus amyloliquefaciens* FZB45 contributes to its plant-growth-promoting effect. *Microbiology* **148**:2097–2109.
- Kelly, W. L., L. Pan, and C. Li. 2009. Thiostrepton biosynthesis: prototype for a new family of bacteriocins. *J. Am. Chem. Soc.* **131**:4327–4334.
- Koumoutsis, A., X.-H. Chen, A. Henne, H. Liesegang, G. Hitzeroth, P. Franke, J. Vater, and R. Borriss. 2004. Structural and functional characterization of gene clusters directing nonribosomal synthesis of bioactive cyclic lipopeptides in *Bacillus amyloliquefaciens* strain FZB42. *J. Bacteriol.* **186**:1084–1096.
- Koumoutsis, A., X.-H. Chen, J. Vater, and R. Borriss. 2007. DegU and YczE positively regulate the synthesis of bacillomycin D by *Bacillus amyloliquefaciens* strain FZB42. *Appl. Environ. Microbiol.* **73**:6953–6964.
- Kunst, F., and G. Rapoport. 1995. Salt stress is an environmental signal affecting degradative enzyme synthesis in *Bacillus subtilis*. *J. Bacteriol.* **177**:2403–2407.
- Le Breton, Y., N. P. Mohapatra, and W. G. Haldenwang. 2006. In vivo random mutagenesis of *Bacillus subtilis* by use of TnYLB-1, a *mariner*-based transposon. *Appl. Environ. Microbiol.* **72**:327–333.
- Lee, S. W., D. A. Mitchell, A. L. Markley, M. E. Hensler, D. Gonzalez, A. Wohlrab, P. C. Dorrestein, V. Nizet, and J. E. Dixon. 2008. Discovery of a widely distributed toxin biosynthetic gene cluster. *Proc. Natl. Acad. Sci. U. S. A.* **105**:5879–5884.
- Li, Y. M., J. C. Milne, L. L. Madison, R. Kolter, and C. T. Walsh. 1996. From peptide precursors to oxazole and thiazole-containing peptide antibiotics: microcin B17 synthase. *Science* **274**:1188–1193.
- Liao, R., L. Duan, C. Lei, H. Pan, Y. Ding, Q. Zhang, D. Chen, B. Shen, Y. Yu, and W. Liu. 2009. Thiopeptide biosynthesis featuring ribosomally synthesized precursor peptides and conserved posttranslational modifications. *Chem. Biol.* **16**:141–147.
- Mitchell, D. A., S. W. Lee, M. A. Pence, A. L. Markley, J. D. Limm, V. Nizet, and J. E. Dixon. 2009. Structural and functional dissection of the heterocyclic peptide cytotoxin streptolysin S. *J. Biol. Chem.* **284**:13004–13012.
- Morris, R. P., J. A. Leeds, H. U. Naegeli, L. Oberer, K. Memmert, E. Weber, M. J. LaMarche, C. N. Parker, N. Burren, S. Esterow, A. E. Hein, E. K. Schmitt, and P. Krastel. 2009. Ribosomally synthesized thiopeptide antibiotics targeting elongation factor Tu. *J. Am. Chem. Soc.* **131**:5946–5955.
- Oman, T. J., and W. A. van der Donk. 2009. Insights into the mode of action of the two-peptide lantibiotic haloduracin. *ACS Chem. Biol.* **4**:865–874.
- Pei, J., and N. V. Grishin. 2001. Type II CAAX prenyl endopeptidases belong to a novel superfamily of putative membrane-bound metalloproteases. *Trends Biochem. Sci.* **26**:275–277.
- Rodriguez-Martinez, J. M., A. Briales, C. Velasco, M. C. Conejo, L. Martinez-Martinez, and A. Pascual. 2009. Mutational analysis of quinolone resistance in the plasmid-encoded pentapeptide repeat proteins QnrA, QnrB and QnrS. *J. Antimicrob. Chemother.* **63**:1128–1134.
- Roy, R. S., A. M. Gehring, J. C. Milne, P. J. Belshaw, and C. T. Walsh. 1999. Thiazole and oxazole peptides: biosynthesis and molecular machinery. *Nat. Prod. Rep.* **16**:249–263.
- Schägger, H., and G. von Jagow. 1987. Tricine-sodium dodecyl sulfate-polyacrylamide gel electrophoresis for the separation of proteins in the range from 1 to 100 kDa. *Anal. Biochem.* **166**:368–379.
- Schmidt, E. W., J. T. Nelson, D. A. Rasko, S. Sudek, J. A. Eisen, M. G. Haygood, and J. Ravel. 2005. Patellamide A and C biosynthesis by a microcin-like pathway in *Prochloron didemni*, the cyanobacterial symbiont of *Lissoclonum patella*. *Proc. Natl. Acad. Sci. U. S. A.* **102**:7315–7320.
- Thompson, J. D., D. G. Higgins, and T. J. Gibson. 1994. CLUSTAL W: improving the sensitivity of progressive multiple sequence alignment through sequence weighting, position-specific gap penalties and weight matrix choice. *Nucleic Acids Res.* **22**:4673–4680.
- van Belkum, M. J., R. W. Worobo, and M. E. Stiles. 1997. Double-glycine-type leader peptides direct secretion of bacteriocins by ABC transporters: colicin V secretion in *Lactococcus lactis*. *Mol. Microbiol.* **23**:1293–1301.
- Vater, J., B. Kablitz, C. Wilde, P. Franke, N. Mehta, and S. S. Cameotra. 2002. Matrix-assisted laser desorption/ionization-time of flight mass spectrometry of lipopeptide biosurfactants in whole cells and culture filtrates of *Bacillus subtilis* C-1 isolated from petroleum sludge. *Appl. Environ. Microbiol.* **68**:6210–6219.
- Vetting, M. W., S. S. Hegde, J. E. Fajardo, A. Fiser, S. L. Roderick, H. E. Takiff, and J. S. Blanchard. 2006. Pentapeptide repeat proteins. *Biochemistry* **45**:1–10.
- Viklund, H., and A. Elofsson. 2008. OCTOPUS: improving topology prediction by two-track ANN-based preference scores and an extended topological grammar. *Bioinformatics* **24**:1662–1668.
- Wieland Brown, L. C., et al. 2009. Thirteen posttranslational modifications convert a 14-residue peptide into the antibiotic thiocillin. *Proc. Natl. Acad. Sci. U. S. A.* **106**:2549–2553.